ORIGINAL CONTRIBUTION

Effect of ultrasound on the microstructure of polystyrene in cyclohexane: a synchrotron small-angle X-ray scattering study

Jianling Zhang · Dongxia Liu · Guanying Yang · Buxing Han · Zhonghua Wu

Abstract Synchrotron small-angle X-ray scattering technique has been used to study the effect of ultrasound on the microstructure of polystyrene (PS) in cyclohexane solutions. The results show that the intramolecular radius of gyration (R_g) decreases with ultrasound, indicating the shrinkage and collapse of PS chains. There is an exponential relationship between R_g and the molecular weight of PS (M_w), and the exponent changes from 0.5 to 0.417, as the ultrasound time is increased. This means that the shape of PS chain changes from random coil to shrunken form. The Kratky plots also confirm the shape transformation of PS chains induced by ultrasound. Moreover, the intermolecular correlation length increases with the ultrasound time, which is indicative of the entanglement of PS chains.

Keywords Ultrasound · Polystyrene · Cyclohexane · Synchrotron small-angle X-ray scattering · Microstructure

Introduction

The relationship between the microstructure of polymers in liquid solvents and its environment change has been an interesting subject for many years [1–5]. It is well known that the configuration of polymer chain depends remarkably on solvent quality [6–8]. As the solvency of the solvent is

J. Zhang · D. Liu · G. Yang · B. Han (✉)
Beijing National Laboratory for Molecular Sciences,
Center for Molecular Sciences, Institute of Chemistry,
Chinese Academy of Sciences,
Beijing 100080, People's Republic of China
e-mail: Hanbx@iccas.ac.cn

Z. Wu
Institute of High Energy Physics, Chinese Academy of Sciences,
Beijing 100039, People's Republic of China

decreased, the polymer chain structures can be changed from the random coil to rodlike aggregates. Many experimental techniques have been used to determine the polymer microstructure in liquid solutions, such as fluorescence spectroscopy [8], light scattering [9], small-angle neutron scattering [10], and small-angle X-ray scattering (SAXS) [11]. In particular, SAXS is a powerful technique to study polymer conformation, especially in dilute solutions [12–18]. It can provide structural information of polymer chain in liquid solutions, such as the size, the shape, and the intermolecular interactions.

Ultrasound has become an important tool in chemistry in recent years [19–21]. It has been well known that ultrasonic radiation in liquids has a variety of physical and chemical effects deriving from acoustic cavitation, which can provide a unique method for driving chemical reactions under extreme conditions. Diverse and promising applications of ultrasound have been exploited in polymer chemistry [22–24], such as polymerization, degradation of polymers, and modification of polymer surfaces. The utilization of ultrasound in polymerization can significantly accelerate the polymerization rate, and the polymers produced under sonication have narrower polydispersity but higher molecular weights than those produced under normal conditions [25]. Ultrasound has also been used in degradation of polymers [26]. In addition, as the bubble collapse near a surface results in jets of liquid impinging at high velocity onto the surface, ultrasound also has been utilized to the modification for polymer and polymer surfaces [27].

In this work, the effect of ultrasound on the microstructure of monodisperse polystyrene (PS) in cycolohexane was investigated by SAXS. The results show that the polymer chains shrink, collapse, and entangle by ultrasonication, and the polymer shape transforms from the random coil to shrunken form.

Experimental section

Materials

Monodisperse PS samples ($M_w/M_n \leq 1.08$) were synthesized by Nanjing Chemical Engineering University. Three polymers with the molecular weights of 3,600, 10,000, and 20,000, respectively, were used. The solvent cyclohexane was purchased from Beijing Chemical Factory (>99.5%) and used as received. Each PS sample was dissolved in cyclohexane at room temperature for more than 48 h before the experiments. Complete dissolution of the polymer was confirmed by observing transparency of the solution. The solution concentrations were 5×10^{-4}, 1×10^{-3}, 2×10^{-3}, and 4×10^{-3} g/ml, respectively.

SAXS experiments

SAXS experiments were carried out at Beamline 4B9A at the Beijing Synchrotron Radiation Facility. The SAXS station was located 31 m from the source. The station was equipped with a SAXS camera, a detector, an online data acquisition, a controlling system, and an alignment carriage. The detailed description of the spectrometer was given elsewhere [28]. The data accumulation time was 3 min. The angular range was chosen so as to provide data from $q=0.005$ Å^{-1} to $q=0.3$ Å^{-1}, where the magnitude of the scattering vector is given by $q = 4\pi \sin(\theta/2)/\lambda$ with θ and λ being the scattering angle and the incident X-ray wavelength of 1.54 Å, respectively. The sample-to-detector distance was 1.50 m. In a typical experiment, the PS/cyclohexane solution was treated with high intensity ultrasound (20 kHz, 50 W) for a certain time, during which a circulating water bath was used to maintain the temperature of the bulk solution at 307.7 K (±2 K). Then, the X-ray scattering was recorded.

Data analysis of SAXS

The X-ray scattering from polymer chain includes contributions from both the intermolecular and intramolecular interactions. The scattering function $I(q)$ is given by the product of two factors: the form factor, $P(q)$, which depends solely on the size and shape of the polymer particles; the structure factor, $S(q)$, which accounts for attractive or repulsive interactions between polymer particles [29]. By assuming that the solvent is structureless, the total scattering is:

$$I(q) \doteqdot S(q) \cdot P(q) \tag{1}$$

Aggregation of the polymer particles leads to the increase in the structure factor at low q. However, when the system is sufficiently dilute, interparticle interactions are significantly reduced. In our experiment, as the concentration of polymer solutions is very low, yielding

$S(q)=1$, we can obtain the $P(q)$ directly from scattering curve at low-q range using Debye equation [30]. For the random coil, the form factor is given by the Debye function as:

$$P(q) = \frac{2}{q^4 R_g^4} \left[\exp\left(-q^2 R_g^2\right) + q^2 R_g^2 - 1 \right] \tag{2}$$

The intramolecular correlation defined by R_g for different concentration of the solution is determined by Debye equation at low-q scattering range from 0.005 to 0.01 Å. Moreover, the overall shape of the polymer chain molecule was also analyzed by Kratky plot, i.e., $I(q) \times q^2$ vs q plot.

The intermolecular correlation length for PS/cyclohexane solutions was obtained by Ornstein–Zernike fitting at mid-q range of 0.04 to 0.08 Å [31]:

$$S(q) = \frac{S(0)}{1 + q^2 \xi^2} \tag{3}$$

where $S(0)$ is the scattering intensity at $q=0$, and ξ is the Ornstein–Zernike correlation length. From the Ornstein–Zernike plot, i.e., $1/S(q)$ vs q^2, the correlation length can be evaluated from the slop of the straight line and the value of $S(0)$ by extrapolation.

Results and discussion

Scattering Intensity

As examples, Fig. 1 shows the SAXS curves of the PS/cyclohexane solutions ($M_w=20,000$, [PS]=5×10^{-4} g/ml) after the different ultrasound time. In contrast to the solution without ultrasound, it is found that the scattering intensity of
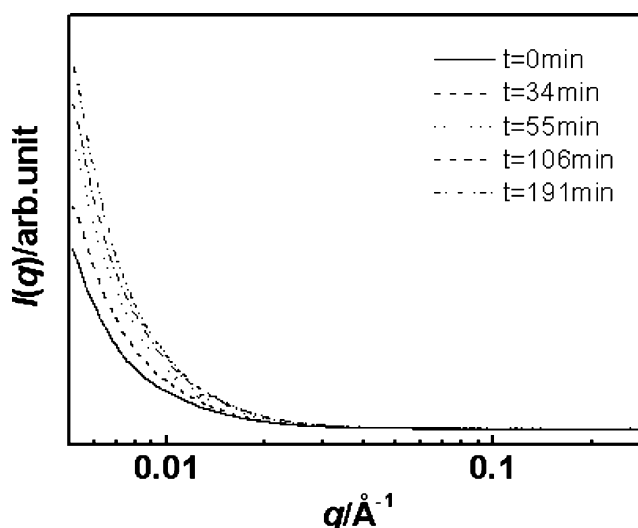

Fig. 1 The experimental SAXS profiles of the PS/cyclohexane solution ($M_w=20,000$, [PS]=5×10^{-4} g/ml) by different ultrasonication time

the solution with the ultrasound is higher, and as the ultrasound time-in belonged, the scattering intensity at low-q range is increased. The scattering in the PS/cyclohexane solution is due to differences in the electron density of the electron-rich polymer chain and the electron-poor solvent. The ultrasound in the solution may cause an increase in the electron density of the polymer phase, which provides better contrast between the polymer and solvent and results in a corresponding increase in the scattering intensity.

Intramolecular radius of gyration

Figure 2 shows the scattering curve of the PS/cyclohexane solutions (M_w=20,000, [PS]=5×10^{-4} g/ml) after the different ultrasound time at low-q range from 0.005 to 0.01 Å and the corresponding Debye fits. The intramolecular radius of gyration R_g for PS at different ultrasound time were determined by extrapolating the R_g at different concentrations to zero concentration, which are shown in Fig. 3. Without the ultrasound, the R_g values of the PS/cyclohexane solutions obtained at M_w of 3,600, 10,000, and 20,000, is 16.1, 27.0, and 37.3 Å, respectively. These values agree well with the unperturbed θ values for PS in cyclohexane of $R_{g-\theta} \approx 0.269 \times M_w^{0.5}$ [32–34]. At 307.7 K, cyclohexane is the θ solvent for PS, and the polymer chains expand with a random coil shape. As we can see from Fig. 3, with the increasing of ultrasound time, the R_g value of PS decreases, indicating that the polymer chains shrink and collapse during the ultrasound process, and it shows that the R_g value decreases drastically in the beginning certain minutes and subsequently decreases less with ultrasound time, which suggests that the effect of ultrasound on the polymer shape is the most remarkable in the beginning certain minutes.
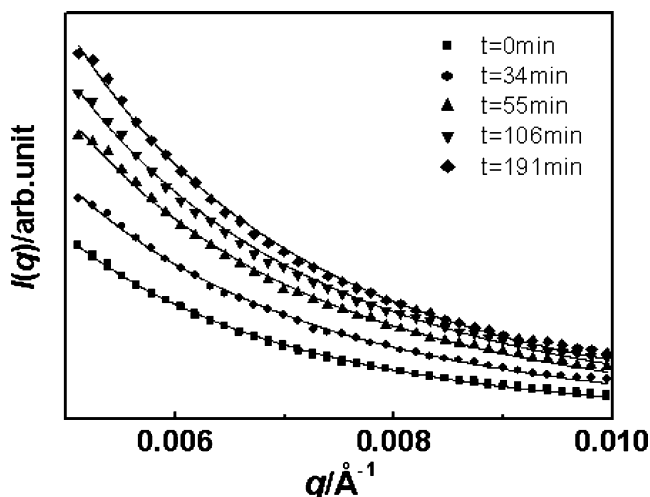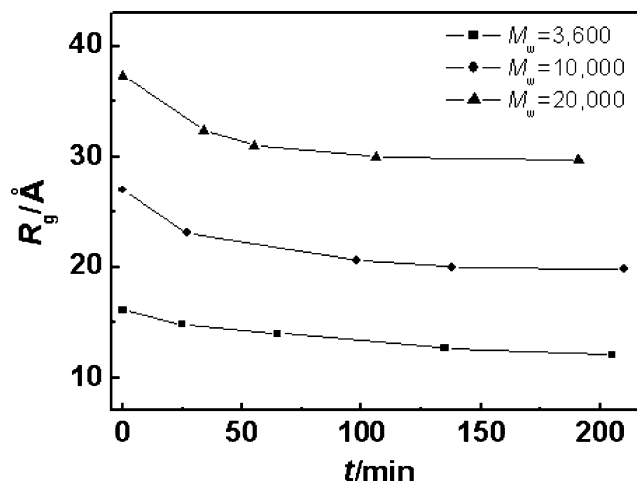

Fig. 3 Gyration radius R_g for PS/cyclohexane solution by different ultrasonication time

The effect of molecular weight M_w on the intramolecular gyration radius R_g at different ultrasound time can be extracted from Fig. 3. If the values of R_g are replotted double-logarithmically against M_w at different ultrasound time, the data point can be fitted by straight line with the power law relationship of $R_g = a \times M_w^b$. The exponent b can provide the information on the microstructure of polymer chains. In the θ solvent, the exponent b is 0.5 characterized of the random coil of polymers. Figure 4 shows the coefficients of a and b in the function of $R_g = a \times M_w^b$ for PS/cyclohexane solution after ultrasonication for various time. As we can see, by increasing the ultrasound time from 0 to 109 min, the exponent b is decreased from 0.5 to 0.417, which means that the PS chains shrink and collapse from random coil. But this shrunken form of PS induced by ultrasound cannot be globular, as it has been predicted that, for the complete globular particles, the exponent b value was
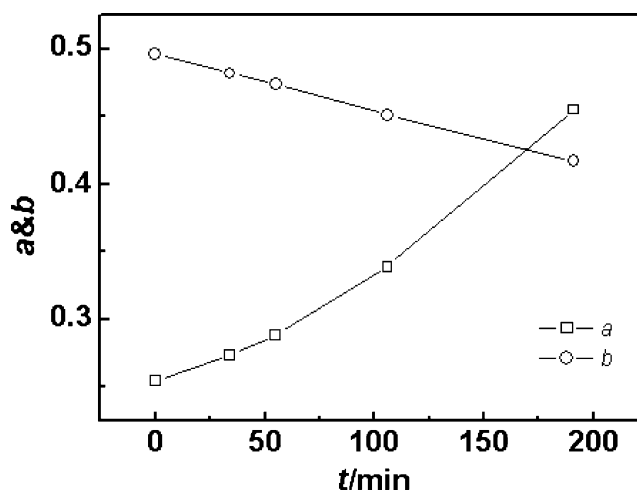

Fig. 2 The experimental SAXS profiles (*solid dots*) and corresponding Debye fits (*solid lines*) for PS/cyclohexane solution (M_w=20,000, [PS]=5×10^{-4} g/ml) by different ultrasonication time

Fig. 4 The coefficient of a and b in the function of $R_g = a \times M_w^b$ for PS/cyclohexane solution by different ultrasonication time

1/3 [35]. It can be concluded that PS exhibits an intermediate structure between the original random coil and globular shape.

Kratky plot

The Kratky plot [$I(q) \times q^2$ vs q] is useful in describing the overall shape of the polymer chain molecule [36–39]. In essence, the Kratky plot shows a clear peak for a globular conformation but has a plateau shape and then increases monotonically for a flexible chain-like molecule. Figure 5 shows the Kratky pattern for PS/cyclohexane solution (M_w=20,000, [PS]=5×10^{-4} g/ml) after ultrasonication for various times. As we can see, without the ultrasound, the Kratky pattern for the PS/cyclohexane solution is monotonically increased, which indicates that the PS chain is in a flexible chain-like conformation. After ultrasonication, evidently, there are some changes for the Kratky pattern. It can be seen from Fig. 5 that the Kratky plot increases gradually in the low-q range and shows a not very clear broaden peak at high-q range. This means that the PS, after ultrasonication, exhibits an intermediate conformation between the original random coil and globular shape [39]. The results from the Kratky plot, together with the estimates of R_g and the relation between M_w and R_g, demonstrate that the PS molecule in cyclohexane has an original expanded flexible chain conformation but has a restricted spatial distribution and a shrunken form induced by the ultrasound.

Intermolecular correlation length

As examples, Fig. 6 shows Ornstein–Zernike plots for PS/cyclohexane solution (M_w=20,000, [PS]=5×10^{-4} g/ml) after ultrasonication for various time. From Ornstein–Zernike plots, the correlation length ξ, which is a measure
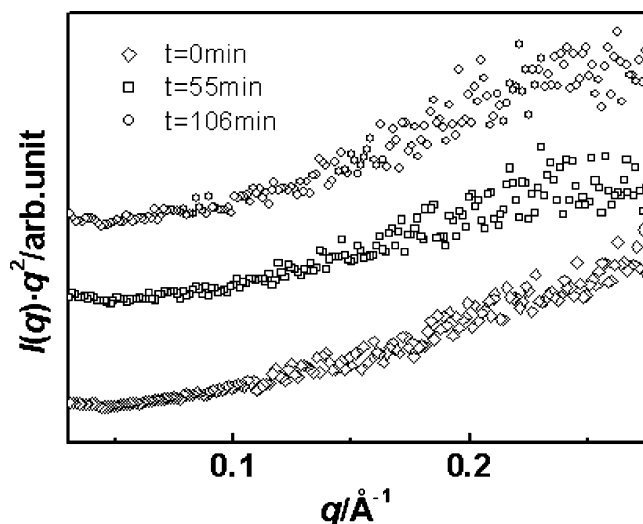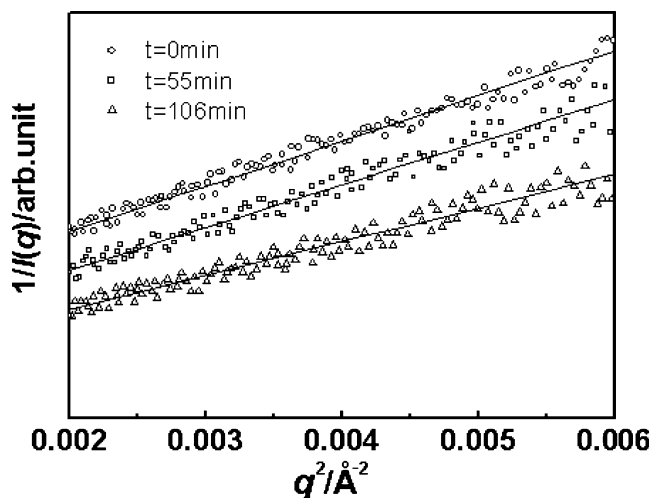

Fig. 6 Ornstein–Zernike plots for PS/cyclohexane solution (M_w=20,000, [PS]=5×10^{-4} g/ml) by different ultrasonication time

of the spatial extent and temporal lifetime of transient, unstable concentration fluctuations of polymer in solutions, can be obtained. Figure 7 shows the dependence of correlation length ξ on ultrasound time. Without the ultrasound, the R_g value obtained by Debye equation for the PS of M_w=3,600, 10,000, and 20,000 is 16.1, 27.0, and 37.3 Å, respectively, and the corresponding correlation length ξ is 9.5, 15.5, and 21.7 Å. The relationship of $\xi_{T_\theta} = R_{g-\theta}/\sqrt{3}$ can be obtained, which is exactly the same as the results obtained by Fujita [40], des Cloizeaux and Jannink [41]. From Fig. 7, it is clear that the correlation length is increased gradually with the increasing ultrasound time, especially in the beginning certain minutes. This indicates that the ultrasound results in an increase in the size and lifetime of transient concentration fluctuation in the PS/cyclohexane solution. The possible reason for this phenomenon is that the ultrasound drives the PS chain to shrink and collapse, which makes the polymer chains closer and leads to a increase in the intermolecular correlation
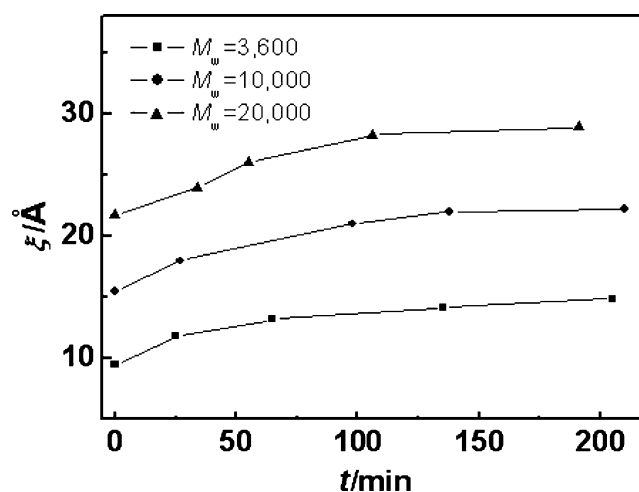

Fig. 5 The Kratky plot for PS/cyclohexane solution (M_w=20,000, [PS]=5×10^{-4} g/ml) by different ultrasonication time

Fig. 7 Correlation length for PS/cyclohexane solution by different ultrasonication time

length. The possible mechanism for the shape change of PS chains in cyclohexane is discussed in the following.

Possible mechanism

The ultrasound-induced microstructure changes of PS in cyclohexane can be explained from the viewpoint of acoustic cavitation: the creation, expansion, and implosive collapse of bubbles in ultrasonically irradiated liquids [42–44]. It has been well known that during cavitation, bubble collapse produces intense local heating, high pressures, and very short lifetimes; these transient, localized hot spots have temperatures of ~5,000°C, pressure of about 1,000 atm, and heating and cooling rates above 10^{10} K/s [19]. Thus, the interfacial region around cavitation bubbles has very large temperature and pressure. In dilute solutions, the polymer chains are in random coil and are free to move in the flow fields around the bubbles. The special temperature and pressure effects of acoustic cavitation could make the polymer chains shrink, collapse, and entangle. In addition, the very large shear and strain gradients in the vicinity of bubbles generated by the very rapid streaming of solvent molecules around the cavitation bubble, as well as the intense shock waves emanated on collapse, may also partly contribute to the shrinkage and entanglement of polymer chains. Moreover, as the ultrasound time is increased, more polymer chains are entangled, which restrict the movement of polymers in the flow field around the bubbles. Therefore, the microstructure change of the polymers is less remarkable at long ultrasound time.

Conclusion

Synchrotron SAXS technique has been used to study the effect of ultrasound on the microstructure of monodisperse PS in solvent of cyclohexane. The intramolecular correlation of the polymer chain decreases with the ultrasound time, and its shape changes from random coil to shrunken form. The Kratky plot also gives further support for the shape transformation of the polymer induced by ultrasound. The correlation lengths between the polymer chains increase with the ultrasound time. This means that ultrasound can cause the entanglement of polymer chains.

References

1. Jejero R, Gomez C, Celda B, Gavara R, Campos A (1998) Makromol Chem 189:1643
2. Raphael E, Pincus P, Fredrickson GH (1993) Macromolecules 26:1996
3. Livadaru L, Kovalenko A (2004) J Chem Phys 121:4449
4. Ericsson CA, Soderman O, Garamus VM, Bergstrom M, Ulvenlund S (2005) Langmuir 21:1507
5. Taylor MP (2004) J Chem Phys 121:10757
6. DiNoia TP, Kirby CF, van Zanten JH, McHugh MA (2000) Macromolecules 33:6321
7. Yang L, Alexandridis P, Steytler DC, Kositza MJ, Holzwarth JF (2000) Langmuir 16:8555
8. Somasundaran P, Kramer G (2004) Colloid Surf A 250:189
9. Zhang J, Wang YM, Liang DH, Ying QC, Chu B (2005) Macromolecules 38:1936
10. DiNoia TP, van Zanten JH, Kline SR, Garach-Domech A, McHugh MA, Wright PJ, Fetters LJ (2003) Macromolecules 36:7372
11. Hanley KJ, Lodge TP, Huang CI (2000) Macromolecules 33:5918
12. Li D, Liu ZM, Han BX, Yang GY, Wu ZH, Liu Y, Dong BZ (2000) Macromolecules 33:7990
13. Li D, Han BX, Liu ZM, Liu J, Zhang XG, Wang SG, Zhang XF, Wang J, Dong BZ (2001) Macromolecules 34:2195
14. Dong BZ, Rong LX, Liu Y, Li D, Han BX, Liu ZM (2003) Sci China Ser G 46:570
15. Abe F, Einaga Y, Yoshizaki T, Yamakawa H (1993) Macromolecules 26:1884
16. Klucker R, Schosseler F (1997) Macromolecules 30:4228
17. Li D, Li ZM, Han BX, Yang GY, Song LP, Wang J, Dong BZ (2002) Macromolecules 35:10114
18. McClain JB, Londino D, Combes JR, Romack TJ, Canelas DA, Betts DE, Wignall GD, Samulski ET, DeSimone JM (1996) J Am Chem Soc 118:917
19. Suslick KS, Price GJ (1999) Annu Rev Mater Sci. 29:295
20. Avivi (Levi) S, Nitzan Y, Dror R, Gedanken A (2003) J Am Chem Soc 125:15712
21. Sakai T, Sakai H, Abe M (2002) Langmuir 18:3763
22. Mayer W, Hoffmann S, Meier G, Alig I (1997) Phys Rev E 55:3102
23. Eckert S, Hoffmann S, Meier G, Alig I (2002) Phys Chem Chem Phys 4:2594
24. Fenner DB (1987) J Chem Phys 87:2377
25. Hiorns RC, Khoukh A, Ghigo P, Prim S, Francois J (2002) Polymer 43:3365
26. Kim H, Lee JW (2002) Polymer 43:2585
27. Sakai T, Sakai H, Abe M (2002) Langmuir 18:3763
28. Dong BZ, Sheng WJ, Yang HL, Zhang ZJ (1997) J Appl Crystallogr 30:877
29. Muroga Y, Yoshida T, Kawaguchi S (1999) Biophys Chemist 81:45
30. Debye P (1946) J Chem Phys 14:636
31. Benoît H, Picot C, Benmouna M (1984) J Polym Sci B 22:1545
32. Lal J, Bansil R (1991) Macromolecules 24:290
33. Cotton JP, Decker D, Benoît H, Farnous B, Higgins J, Jannink G, Ober R, Picot C, Des Cloizeaux J (1974) Macromolecules 7:863
34. Schmidt M, Burchard W (1981) Macromolecules 14:210
35. Nakata M (1971) Makromol Chem 149:99
36. Konno T, Kataoka M, Kamatari Y, Kanaori K, Nosaka A, Akasaka K (1995) J Mol Biol 251:95
37. Konno T, Kamatari Y, Kataoka M, Akasaka K (1997) Protein Sci 6:2242
38. Glatter O, Kratky O (1982) Small-angle X-ray scattering. Academic, New York
39. Tanaka N, Takemura M, Konno T, Kunugi S (1998) Macromolecules 31:8840
40. Fujita H (1990) Polymer solutions. Elsevier, Amsterdam
41. des Cloizeaux J, Jannink G (1990) Polymers in solution: their modeling and structure. Claredon Press, Oxford
42. Flint EB, Suslick KS (1991) Science 253:1397
43. Suslick KS, Hammerton DA, Cline RE Jr (1986) J Am Chem Soc 108:5641
44. Adewuyi YG (2001) Ind Eng Chem Res 40:4681